Hyperfine structure and isotope shift of the D_2 line of $^{76-98}$Rb and some of their isomers

C. Thibault, F. Touchard, S. Büttgenbach,* R. Klapisch, and M. de Saint Simon
Laboratoire René Bernas du Centre de Spectrométrie Nucléaire et de Spectrométrie de Masse, 91406 Orsay, France

H. T. Duong, P. Jacquinot, P. Juncar, S. Liberman, P. Pillet, J. Pinard, and J. L. Vialle
Laboratoire Aimé Cotton, Centre National de la Recherche Scientifique II, 91405 Orsay, France

A. Pesnelle†
CERN, Geneva, Switzerland

G. Huber
Gesellschaft für Schwerionenforschung, D-6100, Darmstadt 1, Germany
(Received 17 October 1980)

Hyperfine structure, spin, and isotope shift measurements have been performed on $^{76-98}$Rb and ^{78,81,82,84,86,90}Rb^m. The Rb nuclei have been produced either by spallation of Nb or by fission of U by a 600 MeV proton beam. They have been separated in mass before being transformed into a thermal atomic beam which interacts at a right angle with the light from a c.w. tunable dye laser. The charge radii changes deduced from the isotope shifts exhibit shell effects at $N = 50$ and deformations at $N = 60$, which are discussed.

[NUCLEAR STRUCTURE $^{76-98}$Rb, ^{78,81,82,84,86,90}Rb^m. Measured hyperfine constants $A(5s\ ^2S_{1/2})$, $A(5p\ ^2P_{3/2})$, $B(5p\ ^2P_{3/2})$; spins, isotope shifts. Deduced μ, Qs, $\delta\langle r^2\rangle$. High resolution laser spectroscopy on thermal atomic beams.]

I. INTRODUCTION

High resolution laser spectroscopy coupled to highly sensitive methods of detection has shown to be very useful for determinations of nuclear spins, nuclear magnetic moments, as well as isotope shift measurements of long series of nuclei of the same element, even for very short-lived ones. Such an experiment has been performed with sodium isotopes of mass number 21 to 31.[1,2] The results that we obtained encouraged us to pursue the systematic study of series of other alkali isotopes. A preliminary experiment has given the structure of the blue D_1 second resonance line of cesium isotopes from mass number 123 up to 137.[3] Another similar experiment has permitted us to observe for the first time the D_2 resonance line of francium[4] and to study the hyperfine structure (hfs) for six of its isotopes.[5]

In the present paper we report on the measurements of hyperfine structure and isotope shifts of rubidium isotopes and isomers from mass number 76 up to 98. A special effort was made to obtain results on ^{97,98}Rb ($N = 60, 61$) as the onset of a sudden deformation for $N \geq 60$ had previously been deduced from the measurement of the atomic masses of these isotopes.[6]

II. EXPERIMENTAL PROCEDURE AND SETUP

The experimental procedure has been extensively described in preceding papers.[1,2,7,8] The experiment rests upon the detection of optical resonances through a magnetic deflection of atoms. In brief, a thermal atomic beam of rubidium interacts at a right angle with the light beam of a tunable single mode c.w. dye laser in the presence of a weak magnetic field parallel to the laser beam (Fig. 1). When tuned at the resonance with one of the hyperfine components of the D_2 line ($5s\ ^2S_{1/2} - 5p\ ^2P_{3/2}$), the laser light may induce an optical pumping which changes the population distribution between the magnetic substates F, m_F, of the ground state. These changes are analyzed by a six-pole magnet[8] according to the value of $m_J = \pm\frac{1}{2}$. The atoms focused by the six-pole magnet are counted by an electron multiplier after they have been ionized and passed through a mass spectrometer. The signal observed while scanning the laser frequency is shown on Fig. 2. From the position of the five observable and well resolved hyperfine transitions (for nuclear spins $I \geq 1$), one can easily deduce the isotope shift as well as the hyperfine constants of the $^2S_{1/2}$ and $^2P_{3/2}$ states, from which the nuclear magnetic moment μ and the electric quadrupole moment Q are determined.[9,10] As described previously, the unknown spins I can be measured by magnetic resonance in a weak static magnetic field.[2]

A. Atomic beam production

The radioactive nuclei are produced either by spallation of niobium or by fission of uranium[11]

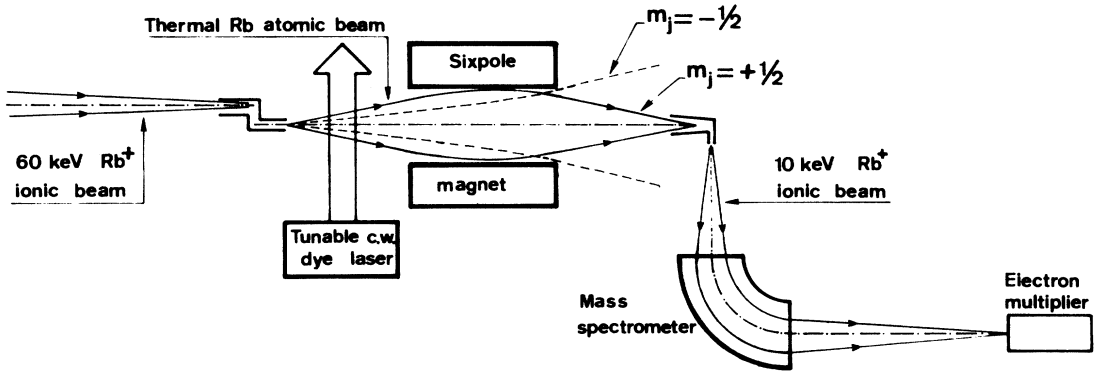

FIG. 1. Schematic view of the experiment. The 60 keV ionic beam from ISOLDE is stopped and neutralized to form a thermal atomic beam which interacts with the light from a tunable c.w. dye laser. The optical pumping, when it occurs, produces changes in population distribution between Zeeman sublevels, which are detected by use of a six-pole magnet. The $m_J = +\frac{1}{2}$ atoms are focused on the input of an ionizer; 10 keV ions are then produced which are passed through the mass spectrometer and counted by the electron multiplier.

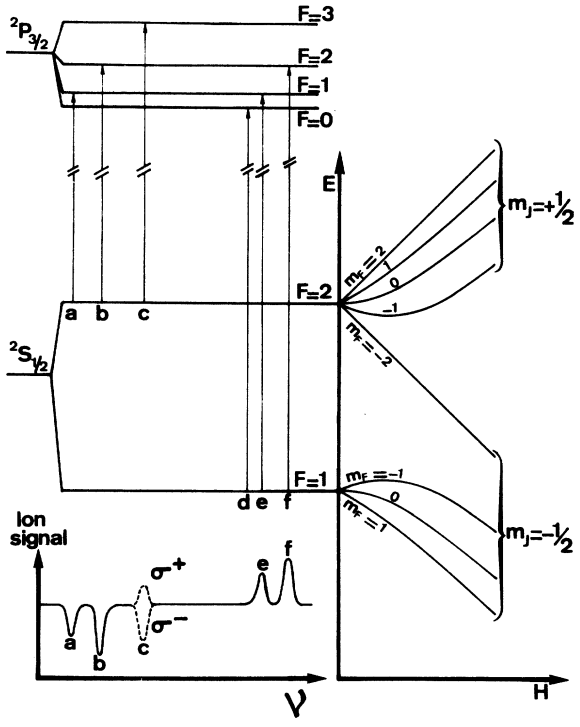

FIG. 2. Signals obtained for the D_2 line when $I=\frac{3}{2}$. The transitions a, b, e, f, induce an optical pumping detected by the six-pole magnet which focuses the $m_J = +\frac{1}{2}$ states. The transition c can be detected through Zeeman pumping by use of σ^+ or σ^- polarized light in the presence of a weak magnetic field. For σ^+ or σ^- polarization the Zeeman pumping favors the upper (lower) m_F level and finally produces a positive (negative) signal. The transition d, which does not undergo any optical pumping, cannot be observed by the used magnetic detection. These five transitions can be observed for $I \geq 1$.

(Fig. 3), both induced by the 600 MeV protons delivered by the CERN synchrocyclotron (SC). The atoms are mass separated by the on-line separator ISOLDE which provides a 60 keV monoionic beam. It is converted into a thermal atomic beam through a special device (Fig. 4); the ions are implanted onto a tantalum surface heated at 1200 °C and then reemitted as thermalized ions. The heating voltage directs these ions towards a tubular region

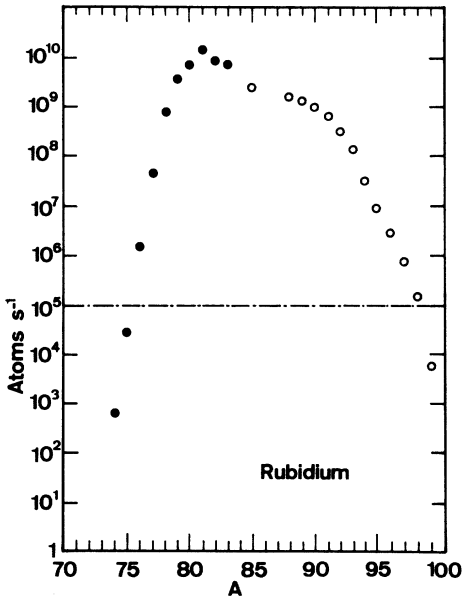

FIG. 3. ISOLDE production yields of rubidium isotopes obtained by spallation of niobium (full circles) or by fission of uranium (empty circles) using the 0.8 μA beam of 600 MeV protons from the SC at CERN. Noise considerations as well as the sensitivity of our technique of detection allowed us to study all isotopes produced at a higher rate than 10^5 atoms/s.

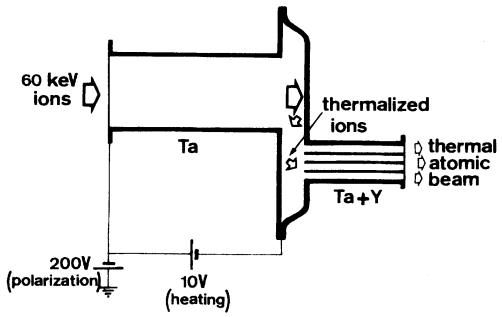

FIG. 4. Special device used to transform the 60 keV ions from ISOLDE into a thermal atomic beam. The ions are first thermalized and finally neutralized when remitted by the Ta+Y surface of the output tubes.

made of tantalum coated with yttrium. Because of the low work function of yttrium, the ions can be neutralized there. In addition, a static potential of about 200 V confines the ions inside the tube so that only atoms can be evaporated out of the device. From geometrical considerations, the efficiency of the neutralization has been estimated to be better than 80% for a desorption time of 150 ms (half-maximum).

B. Laser system

Basically, the laser system is the same as the one used during former experiments.[2] It is a commercial c.w. tunable dye laser (CR 599) oscillating on one single mode whose frequency is servo-controlled and scanned step by step by a "sigma-meter"[2,12] which is itself stabilized using a He-Ne laser locked on an iodine saturated absorption line. As the D_2 line of rubidium is located at wavelength $\lambda = 780.0$ nm, the proper dye to be used is the so-called "DEOTC" dissolved in ethylglycol mixed with 10% of dimethylsulfoxyde (DMSO). The dye molecules are excited by the strong red lines of a Kr^+ laser (CR 3000 K). Using about 4 W of pumping power, the single mode operation is generally achieved at a power level of 30 mW.

C. Data acquisition

As explained the observable transitions do not appear on a zero background but as positive or negative peaks relative to a mean ionic current. It is thus necessary to use a normalization procedure in order to get rid of the fluctuations of this mean current. To do so, the light is alternately switched on and off every 0.5 s. The two signals—with and without light—are recorded alternately during 0.4 s and stored into different buffer counters. The difference between the two signals provides a good normalization, as can be seen on Fig. 5. Two other buffer counters are used to record the fluorescence signal of an auxiliary atomic beam of natural rubidium and a measurement of the relative frequency of the light given by the sigma-meter. All the data are transferred to a PDP 9 computer and recorded on magnetic tapes. Complete structures and relative positions of all isotopes and isomers which have been studied are displayed in Fig. 6.

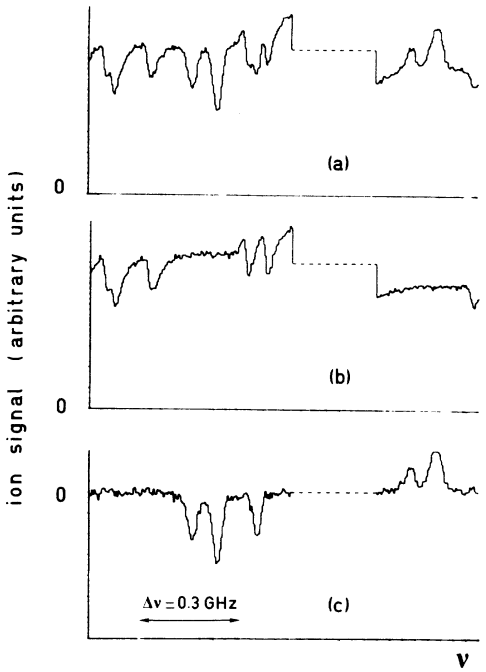

FIG. 5. Example of normalization of the data showing the five observable components of the D_2 line of ^{93}Rb. (a) Spectrum with light, (b) spectrum without light, (c) normalized spectrum obtained as the difference $a - b$.

III. RESULTS

A. Spins

The unknown spins of isotopes ^{86}Rb^m, ^{96,97}Rb have been measured. The spin of ^{98}Rb is probably zero since only one resonance, located very close to the expected center of gravity, has been observed. All the values are reported in Table I.

B. Magnetic moments

For each component of the resonance line, the center of gravity of the peak has been calculated and Zeeman shifts have been taken into account. The values of the A factor for the $^2S_{1/2}$ state and of A and B for the $^2P_{3/2}$ state have been deduced from the position of the resonances through a least-square-fit adjustment. All results are reported in Tables I and II as well as results from other experiments. Within the experimental error limit no hyperfine anomaly has been observed; the

TABLE I. Values of the spins and hyperfine constants $A(5s\ ^2S_{1/2})$ measured in this work and in others, and deduced values of the magnetic moments of the studied nuclei.

A	$T_{1/2}$	I	$A(5s\ ^2S_{1/2})$ (MHz) This work	Other results	μ (μ_N) This work
76	39 s	1	−701 (17)		−0.376 (9)
77	3.8 min	$\frac{3}{2}$	815.7 (5.1)	812.5 (3.4)[b]	0.656 8 (41)
78	17.5 min	0			
78m	6.3 min	4	1186.8 (1.0)	1195 (6)[b]	2.548 5 (21)
79	23 min	$\frac{5}{2}$	2502.0 (0.9)	2511 (9)[b]	3.357 9 (12)
80	30 s	1	−155.2 (3.2)	−155.957 (2)[c]	−0.083 3 (17)[h]
81	4.58 h	$\frac{3}{2}$	2557.6 (1.7)	2555.795 (20)[d,e]	2.059 5 (14)
81m	32 min	$\frac{9}{2}$	2317.3 (0.7)		5.598 0 (17)
82	1.25 min	1	1031 (10)	1031.6 (1.1)[c]	0.553 6 (54)
82m	6.2 h	5	563.6 (0.9)	562.560 48 (6)[d,e]	1.513 3 (24)
83	86.2 d	$\frac{5}{2}$	1061.7 (0.6)	1061.1 (1.9)[d,e]	1.424 9 (8)
84	33 d	2	−1233.7 (1.5)	−1233.264 (2)[d,e]	−1.324 6 (16)
84m	20.4 min	6	68.2 (4.6)		0.220 (15)
85	stable	$\frac{5}{2}$	1011.0 (1.0)	1011.910 813 (2)[d,e]	1.357 0 (10)
86	18.65 d	2	−1581.2 (1.5)	−1578.753 (1)[d,e]	−1.697 7 (16)
86m	1.018 min	6[a]	563.5 (0.3)		1.815 0 (10)
87	4.9×10^{10} yr	$\frac{3}{2}$	3415.9 (2.0)	3417.341 307 (1)[d,e]	2.750 6 (10)
88	17.7 min	2	476.6 (2.4)	±474.434 (7)[d,e]	0.511 7 (26)
89	15.4 min	$\frac{3}{2}$	2960.1 (0.9)	2964 (5)[f]	2.383 6 (7)
90	3.03 min	0			
90m	4.26 min	3	1003.4 (0.4)	1004.6 (3.4)[f]	1.615 98 (64)
91	58.0 s	$\frac{3}{2}$	2709.1 (1.7)	2712.5 (4.0)[f]	2.181 5 (15)
92	4.48 s	0			
93	5.85 s	$\frac{5}{2}$	1050.2 (1.2)	1047 (4)[g]	1.409 5 (16)
94	2.73 s	3	930.4 (1.1)		1.498 4 (18)
95	0.38 s	$\frac{5}{2}$	993.7 (2.5)		1.333 6 (34)
96	0.20 s	2[a]	1365.2 (1.6)		1.465 8 (17)
97	0.17 s	$\frac{3}{2}$[a]	2286.2 (2.6)		1.841 0 (21)
98	0.11 s	[0][a]			

[a] This work.
[b] See Ref. 41.
[c] R. Neugart, private communication.
[d] See Ref. 13.
[e] See Ref. 14.
[f] See Ref. 42.
[g] W. Klempt, J. Bonn, and R. Neugart, Phys. Lett. 82B, 47 (1979).
[h] A direct measurement has also been performed by R. Neugart *et al.* (see c), which provides $\mu = -0.0836\ (6)\ \mu_N$.

TABLE II. Values of the hyperfine constants $A(5p\ ^2P_{3/2})$ and $B(5p\ ^2P_{3/2})$ measured in this work and in others, and deduced spectroscopic quadrupole moments for the studied nuclei.

A	$A(5p\ ^2P_{3/2})$ (MHz) This work	$B(5p\ ^2P_{3/2})$ (MHz) This work	Other results	Q_s (b) This work
76	−18.0 (10.5)	36.0 (14.1)		0.38 (0.15)
77	19.1 (1.5)	65.3 (3.0)		0.695 (32)
78				
78*m*	29.4 (0.5)	76.5 (3.7)		0.814 (39)
79	62.0 (0.4)	−9.2 (2.1)		−0.098 (22)
80	−1.8 (2.3)	32.7 (1.9)		0.348 (20)
81	63.8 (0.8)	37.4 (2.2)		0.398 (23)
81*m*	57.9 (0.4)	−69.8 (5.4)		−0.743 (57)
82	26.8 (3.2)	17.9 (6.8)		0.190 (72)
82*m*	14.0 (0.6)	94.6 (11.2)		1.01 (0.12)
83	26.5 (0.4)	18.4 (2.1)	24 (9)[a]	0.196 (22)
84	−30.1 (0.8)	−1.4 (3.3)	0.0 (1.9)[a]	−0.015 (35)
84*m*	1.2 (1.0)	54 (26)		0.57 (0.27)
85	25.3 (0.4)	21.4 (4.0)	26.032 (70)[b]	0.228 (43)
86	−39.0 (0.8)	18.1 (3.0)	18.6 (2.8)[a]	0.193 (32)
86*m*	14.3 (0.4)	34.7 (8.9)		0.369 (95)
87	84.29 (0.50)	12.2 (2.0)	12.611 (70)[b]	0.130 (21)
88	9.4 (2.3)	−1.1 (9.0)		−0.012 (96)
89	72.6 (1.1)	13.5 (2.4)		0.144 (26)
90				
90*m*	25.3 (0.4)	19.2 (4.2)		0.204 (45)
91	66.9 (1.1)	14.5 (2.4)		0.154 (26)
92				
93	25.8 (0.7)	16.6 (3.8)		0.177 (40)
94	23.2 (0.6)	15.3 (4.7)		0.163 (50)
95	24.0 (0.9)	19.8 (6.1)		0.211 (65)
96	32.9 (1.3)	23.1 (5.3)		0.246 (56)
97	55.2 (1.8)	54.6 (4.1)		0.581 (44)
98				

[a] See Ref. 35.
[b] See Ref. 13.

ratio $A(^2S_{1/2})/A(^2P_{3/2})$ is found to be fairly constant. All magnetic moments deduced from the measurements of $A(^2S_{1/2})$ are reported in Table I. The following well known formula has been used:

$$\frac{\mu^x}{I^x}=\frac{\mu^{87}}{I^{87}}\ \frac{A(^2S_{1/2})^x}{A(^2S_{1/2})^{87}}$$

with

$$A(^2S_{1/2})^{87}=3417.341\,307(2)\ \text{MHz (Ref. 13)},$$

$$\mu^{87}=2.751\,816(2)\ \mu_N\ \text{(Ref. 14)},$$

$$I^{87}=\tfrac{3}{2}\ .$$

Our experimental method also gives the sign of the magnetic moment.

C. Quadrupole moments

The spectroscopic quadrupole moment Q_{hfs} is deduced from the measured value of $B(^2P_{3/2})$ through the usual formula

$$B=\frac{2}{5}\frac{e^2Q_{\text{hfs}}}{hc}\langle r_e^{-3}\rangle R_\tau\ (\text{cm}^{-1})\ .$$

According to the study made in Ref. 15 which shows that the Hartree-Slater calculation gives the best results for magnetic moments of rubidium isotopes, we have used the $\langle r_e^{-3}\rangle$ value given there for the $5p$ level, taking into account the relativistic correction R_τ: $\langle r_e^{-3}\rangle R_\tau=0.796$ a.u. Antishielding correction[16] has also been applied to all final values Q_s in Table II, using

$$Q_s=\frac{1}{1-R}Q_{\text{hfs}}=0.796Q_{\text{hfs}}=1.064\times10^{-2}B$$

with B in MHz and Q_s in barns. To obtain the intrinsic quadrupole moment of the nucleus (Q_0) from the measured static quadrupole moment (Q_s) we use the projection formula[9]

$$Q_0=\frac{(I+1)(2I+3)}{I(2I-1)}Q_s\ .$$

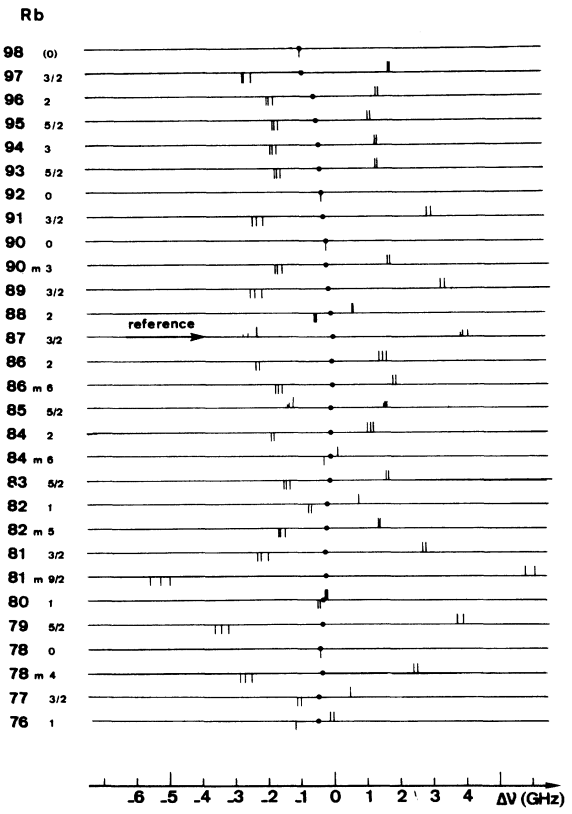

FIG. 6. Complete structures and relative positions of all studied isotopes and isomers. The different nuclei are indicated with their mass number (m is for an isomer) and with their measured nuclear spin. The dots represent the center of gravity of the line structures. For the stable isotopes (mass number 85 and 87), because of the fluorescence detection, all components appear as positive ones.

This formula is expected to hold only in the case of axially symmetric and strongly deformed nuclei.

D. Isotope shifts

From the determination of the hfs constants and spins, it is straightforward to deduce the position of the center of gravity of the D_2 line of an isotope A, which is compared to the one of the reference spectrum of isotope A' simultaneoulsy recorded, i.e., ^{87}Rb. The results are reported in Table III. The quoted errors take into account the consistency between the results obtained from each hyperfine component of the line. By subtracting from the observed isotope shift $\Delta\nu^{AA'}$ the normal mass shift[9,10] $\Delta\nu_{nms}$ and taking a zero value for the specific mass shift $\Delta\nu_{sms}$ (see below) one obtains the volume shift $\Delta\nu_{vol}^{AA'}$ reflecting the change in the mean square radius $\delta\langle r^2\rangle$ of the nuclear charge distribution. The proportionality between $\Delta\nu_{vol}^{AA'}$ and $\delta\langle r^2\rangle^{AA'}$ is given by a factor F (Ref. 17):

TABLE III. Values of the measured isotope shifts and deduced variations of the mean square charge radius of the studied nuclei using $\Delta\nu_{sms}=0$ and $F=-650$ MHz/fm^2.

	$\delta\nu^{A-87}$		$\delta\langle r^2\rangle^{A-87}$	
	This work	Other work	This work	Other work
76	−494 (17)		0.220 (27)	
77	−498.6 (4.5)		0.2831 (69)	
78	−478.4 (1.5)		0.3060 (23)	
78m	−403.8 (1.7)		0.1912 (26)	
79	−391.6 (1.5)		0.2249 (23)	
80	−352.8 (4.4)		0.2166 (68)	
81	−289.9 (1.4)		0.1698 (22)	
81m	−270.4 (1.4)		0.1398 (22)	
82	−233.7 (4.2)		0.1322 (65)	
82m	−233.5 (3.8)		0.1319 (58)	
83	−150.1 (1.0)		0.0512 (15)	
84	−91.6 (2.1)		0.0078 (32)	
84m	−84 (10)		0.004 (16)	
85	−80.1 (1.4)	−75.2 (3.0)[a]	0.0355 (22)	0.0279 (46)[a]
		−79.8 (3.0)[b]		0.0350 (46)[b]
86	−45.8 (2.0)		0.0271 (31)	
86m	−32.1 (2.3)		0.0060 (35)	
87	0		0	
88	−61.0 (5.1)		0.1364 (78)	
89	−143.7 (2.0)		0.3051 (31)	0.313 (12)[c]
90	−197.7 (5.2)		0.4289 (80)	0.418 (12)[c]
90m	−188.6 (2.0)		0.4149 (31)	
91	−255.8 (2.3)		0.5580 (35)	0.564 (12)[c]
92	−320.4 (5.2)		0.6963 (80)	0.685 (12)[c]
93	−371.5 (2.1)		0.8130 (32)	0.797 (12)[c]
94	−414.7 (2.3)		0.9167 (35)	
95	−495.9 (3.8)		1.0781 (56)	
96	−528.3 (4.8)		1.1637 (74)	
97	−879.7 (4.0)		1.7391 (62)	
98	−910 (10)		1.821 (15)	

[a] See Ref. 21.

[b] J. R. Beacham and K. L. Andrew, J. Opt. Soc. Am. 61, 231 (1971).

[c] W. Klempt, J. Bonn, and R. Neugart, Phys. Lett. 82B, 47 (1979). The values in this table have been calculated using $F=-650$ MHz/fm^2 instead of $F=-690$ MHz/fm^2.

$$\Delta\nu_{vol}^{AA'}=F\times\delta\langle r^2\rangle^{AA'}$$

with

$$F=\frac{\pi a_0^3}{Z}\times\beta_s\times|\Psi_s(0)|^2\ f(Z)\ .$$

β_s is a screening factor due to the change in the wave functions of the inner closed shell electrons induced by the valence electron as it changes from $5s$ to $5p$. It has been calculated for Na (Ref. 18) and Cs.[19] As both values are found to be equal to 1.1, we have adopted this value for Rb too. A nonrelativistic value for the charge density $|\Psi_s(0)|^2$ of the $5s$ electron at the nucleus has been extracted from the ground state hyperfine structure of ^{85}Rb (Ref. 9): $|\Psi_s(0)|^2=2.05\ a_0^{-3}$. $f(Z)$, which

takes into account the relativistic corrections to $|\Psi_s(0)|^2$ as well as the finite nuclear charge distribution, has been calculated using a formula derived by Babushkin,[20] as $f(Z) = -3398$ MHz/fm^2. Finally one obtains $F = -650$ MHz/fm^2. The values obtained for $\delta\langle r^2\rangle$, taking ^{87}Rb as a reference, are reported in Table III.

The assumption that $\Delta\nu_{sms} \sim 0$ was made *a priori* following the discussion by Brechignac *et al.*,[21] who suggested that it might be very similar to that of Sr II which is known to be very small (-0.05 $\Delta\nu_{sms}$). It is confirmed *a posteriori* since Fricke and his collaborators have recently performed an absolute measurement of the charge radii of the natural rubidium isotopes. They have found, as a preliminary value, $\delta\langle r^2\rangle^{85-87} = 0.037$ fm^2,[22] which is in excellent agreement with the value that we have obtained (0.036 fm^2) using $\Delta\nu_{sms} = 0$.

The variation of $\delta\langle r^2\rangle^{A-87}$ versus neutron number N is shown on Fig. 7. Clearly this plot exhibits three different regions corresponding to the neutron numbers $N \leq 50$, $50 < N < 60$, and $N \geq 60$. For $N = 50$ one observes a drastic change in the slope of the curve, while at $N = 60$ a sudden jump occurs. These two features will be discussed in detail below.

IV. DISCUSSION

The normal behavior expected for $\langle r^2\rangle$ is an increase with mass number A. However on Fig. 7, from ^{78}Rb to ^{87}Rb—i.e., up to the closure of the neutron shell at $N = 50$—the mean square radius $\langle r^2\rangle$ of the nuclear charge distribution decreases when neutrons are added. Such a trend had already been observed for stable Kr isotopes from $N = 42$ to 50 (Ref. 23) and for $^{85\text{-}87}$Rb.[21] It also occurs for calcium isotopes when filling up the neutron shell at $N = 28$.[24-26] These variations of $\langle r^2\rangle$ reflect both the changes in volume of the nucleus when neutrons are added and the departures from spherical symmetry.

For a spherical nucleus having approximately the same number of protons and neutrons, the charge radius may be expressed using the standard formula where the nucleus is considered as a liquid drop:

$$\langle r^2\rangle_{sph} = \langle r^2\rangle_{std} = \tfrac{3}{5}(r_0 A^{1/3})^2,$$

with $r_0 = 1.2$ fm. In the case of a quadrupole deformation at constant volume, characterized by the parameter β, one has

$$\langle r^2\rangle = \left(1 + \frac{5}{4\pi}\langle\beta^2\rangle\right)\langle r^2\rangle_{sph}.$$

The total change in $\langle r^2\rangle$ between two neighboring isotopes can be expressed as

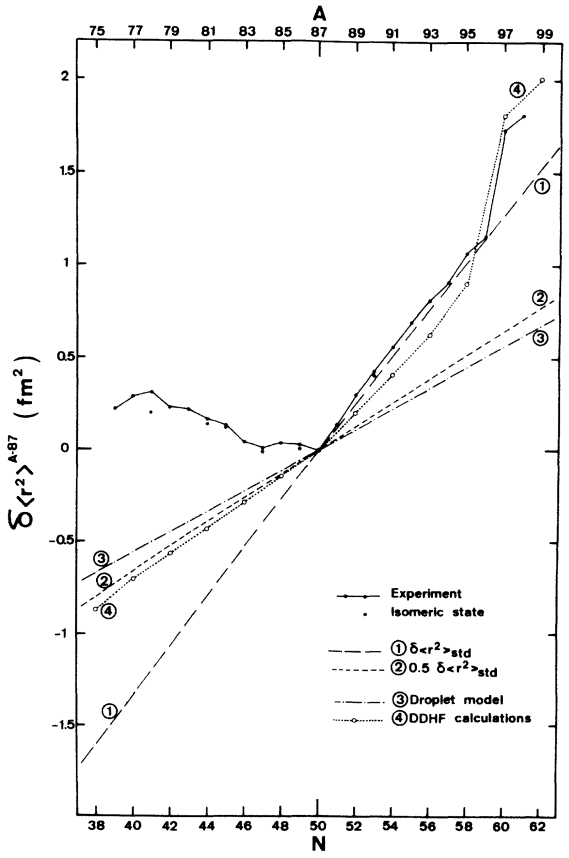

FIG. 7. Variation of the mean square nuclear charge radius relative to ^{87}Rb. The experimental values are compared to values from the standard formula (1) and its derived formula with $\rho = 0.5$ (2), from the droplet model (3), and from DDHF calculations (4).

$$\delta\langle r^2\rangle = \delta_{sph}\langle r^2\rangle + \frac{5}{4\pi}\delta(\langle\beta^2\rangle\langle r^2\rangle_{sph})$$
$$= \delta_{sph}\langle r^2\rangle + \delta_\beta\langle r^2\rangle .$$

However, as we are dealing with the mean square value of the charge radius a nonzero value of $\langle\beta^2\rangle$ may also correspond to dynamical vibrations of the nucleus.

In order to extract $\delta_\beta\langle r^2\rangle$ from the observed $\delta\langle r^2\rangle$ variation, first one has to evaluate $\delta_{sph}\langle r^2\rangle$. The simplest way would be to follow the standard formula and to use

$$\delta_{sph}\langle r^2\rangle = \delta\langle r^2\rangle_{std}$$
$$= \frac{2}{3}\frac{\delta A}{A}\langle r^2\rangle_{std}.$$

However, this formula holds only if neutrons and protons are added together. When neutrons only are added, it is well known that $\langle r^2\rangle$ increases more slowly. This is generally taken into account[27] by assuming that

$$\delta_{sph}\langle r^2\rangle = \rho\delta\langle r^2\rangle_{std},$$

with $0<\rho<1$, and experiment shows that $\rho\sim0.5$ gives a good overall fit. Another possibility for evaluating $\delta\langle r^2\rangle$ is to use the values of R_z obtained by Myers in the droplet model.[28]

All these $\delta_{sph}\langle r^2\rangle$ evaluations are nearly linear with δA. On Fig. 7, $\delta_\beta\langle r^2\rangle$ is the difference between the experimental data and the values of $\delta_{sph}\langle r^2\rangle$ deduced by the preceding formulas. In the simple model of odd-even and odd-odd Rb nuclei, the odd protons and neutrons are moving around the corresponding Kr core. The root mean square deformation β_{rms} indicating deformation or vibration amplitude for Kr and Sr nuclei are calculated either from $B(E_2)$ measurements[29] as in Ref. 30 or, when not available, from E_{2^+} values[29] through the Grodzins formula.[31] Figure 8 shows the plot of the values obtained versus the neutron number N. The deformation trend in the sequence of Rb nuclei is expected to be similar. Therefore it is possible to estimate $\delta_\beta\langle r^2\rangle$. It thus appears that it is impossible to fit the experimental results in both regions—before and after the shell closure—by a unique formula for $\delta_{sph}\langle r^2\rangle$. As shown in Fig. 9, a good agreement may be obtained by using $\rho\sim0.25$ for $N<50$ and $\rho\sim0.8$ for $N>50$. This means that even for spherical nuclei the closure of the neutron shell induces a strong change of the slope of $\delta\langle r^2\rangle^{A-87}$.

Qualitative indications of this shell effect had been found in a systematic study of experimental rms charge radii by Angeli *et al.*[32] However neither the semi-empirical models[27,28] nor the recent *ab initio* calculations performed by Angeli *et al.*[33]

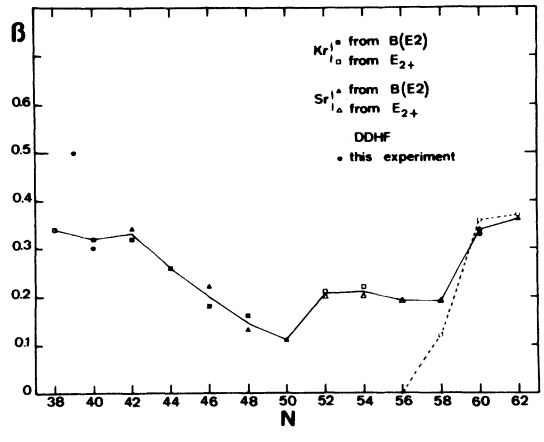

FIG. 8. Values of the deformation parameter β for Kr and Sr isotopes versus N. The experimental values are deduced either from $B(E_2)$ or E_{2^+} measurements in even-even isotopes and compared to the values calculated by the DDHF method. The values deduced from our measurements for ^{76,77,97}Rb are also indicated (see text for discussion).

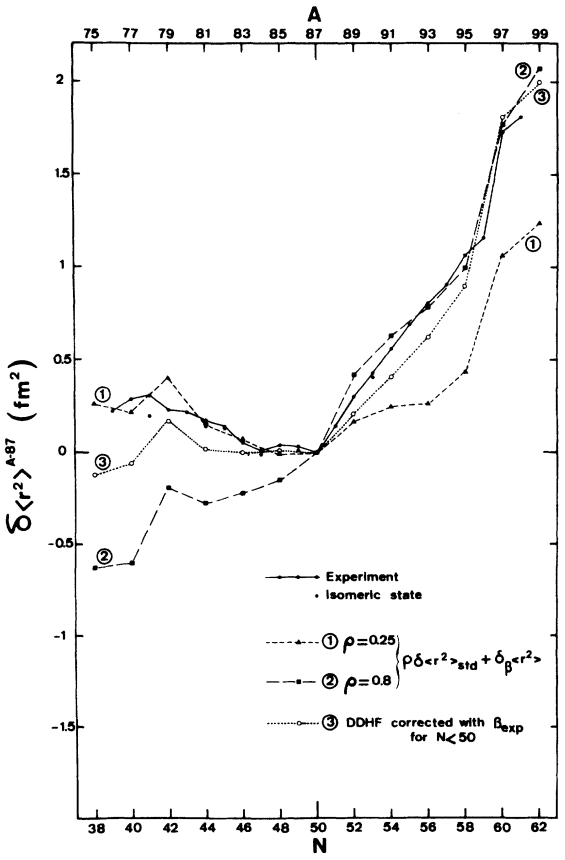

FIG. 9. Variation of the mean square nuclear charge radius relative to ^{87}Rb. The modified standard formula corrected by taking into account the experimental β values is shown for $\rho=0.25$ and $\rho=0.8$, which, respectively, best fits the experimental data in the region below or above $N=50$. The DDHF calculation corrected for $N<50$ is also shown.

include any shell effect. A more sophisticated treatment is thus needed. Since our measurements, Campi and Epherre have performed *ab initio* density dependent Hartree-Fock calculations (DDHF) for even-even Kr and Sr isotopes.[34] Rotational deformations are included in such calculations but not the vibrations. The agreement is quite good for $N>50$ (Fig. 7) while for $N<50$ both $\delta\langle r^2\rangle$ and β values disagree (Figs. 7 and 8). The DDHF calculation gives $\beta=0$ for $N<50$ while the experimental β values are not zero. Therefore the calculated $\delta\langle r^2\rangle$ values may be corrected as was done for the semi-empirical laws. The resulting curve reported on Fig. 9 fits relatively well all the experimental values, showing that the shell effect for spherical nuclei is well indicated by the DDHF method. Campi and Epherre suggested that the experimental β values were not reproduced for $N<50$ by DDHF because they are due to

zero point quadrupolar vibrations. Indeed a vibrational behavior has already been established for $N=46-49$.[35] For lower values of N, the situation is more intricate. Quasirotational bands are observed in many cases together with β values around 0.3 indicating transitional nuclei for $N=40-42$.[36] A region of strong deformation could even exist around $N=38$.[37] If we apply the projection formula to the Q_s values obtained for the lightest isotopes, i.e., ^{77,76}Rb, we obtain, respectively, $\beta_{rms}=0.45$ and 0.5. These very high values could indicate that ^{77,76}Rb are strongly deformed rotational nuclei. However, it does not seem to be the case for their isotones ^{74}Kr and ^{76}Kr or ^{78}Sr since β is smaller (~0.33) and E_{4^+}/E_{2^+} is only 2.5 (Ref. 29) instead of 3.3 for a pure rotor.

For $N \geq 60$ the onset of a large deformation already deduced from the Rb mass measurements[6] is clearly confirmed. While from $N=50$ to 59, the nuclei are nearly spherical and exhibit a smooth increase of $\langle r^2 \rangle$, the observed variation between $N=59$ and 60 is about 10 times larger than the neighboring differences. Such a deformation has also been observed in this region for the Sr isotopes by E_{2^+}, E_{4^+}, and $B(E_2)$ measurements. The values of the ratio E_{4^+}/E_{2^+} for $^{98}Sr_{60}$ (3.0) (Ref. 38) and $^{100}Sr_{62}$ (3.2) (Ref. 39) are very near the theoretical one (3.3) corresponding to a pure rotational structure. As a consequence, the value of the projecting factor for Q_s has to be right for ^{97}Rb. This is verified since we obtain $\beta=0.33$, while $B(E_2)$ measurements[39] provide $\beta=0.34$ for ^{98}Sr and $\beta=0.36$ for ^{100}Sr.

This rotational deformation is well reproduced by DDHF calculation which provides $\beta=0.36$ for $N=60$ and fits quite well the $\delta\langle r^2 \rangle$ jump (Fig. 7). It has also been found by the shell correction method developed by Ragnarsson[40] who has estimated $\beta=\pm 0.35$ ($\epsilon=0.3$).

By combining the different information that we obtained (I, μ, β), it may thus be possible to assign the corresponding Nilsson orbitals if these are not too mixed. This analysis has been performed for $^{77-95}$Rb by Ekström[41,42] using the known I and μ values. However, the case of ^{97}Rb is particularly interesting since we have measured I, μ, and Q_0 and one knows that it must correspond to a pure deformed Nilsson orbital. Using the particle + rotor model, Ragnarsson[40] has calculated μ for the different Nilsson orbitals corresponding to $I=\frac{3}{2}$ and $\epsilon=0.29$ (i.e., $Q_s=0.6$ b). He has obtained $\mu=0.7\ \mu_N$ for $[312,\frac{3}{2}]$, $\mu=1.9\ \mu_N$ for $[301,\frac{3}{2}]$, and $\mu=1.99\ \mu_N$ for $[431,\frac{3}{2}]$. Comparing those to $\mu_{exp}=1.84\ \mu_N$, the orbital $[312,\frac{3}{2}]$ is excluded. In order to choose between the two others, as a strong gap is found between them for $\epsilon=0.3-0.4$ (Ref. 40), the lower orbital $[431,\frac{3}{2}]$ seems to be much more probable.

V. CONCLUSION

These measurements covering a very long series of Rb isotopes allowed us to point out and to document the following different interesting nuclear features.

(i) The closure of the neutron shell at $N=50$ has an effect upon the $\delta\langle r^2 \rangle$ variation even for spherical nuclei; $\langle r^2 \rangle$ increases more rapidly when the neutrons start filling a new shell than when the shell is nearly closed.

(ii) A variation of $\delta\langle r^2 \rangle \sim A^{-87}$ inverse of the one of A is observed before the closure of the neutron shell at $N=50$. This is due partly to the shell effect for spherical nuclei and partly to the existence of a deformation which could be vibrational.

(iii) The nuclei of the region $50<N<60$ are not far from spherical.

(iv) A large purely rotational deformation arises for $N=60$ which is very clearly revealed by a strong increase of $\delta\langle r^2 \rangle$ between $N=59$ and 60.

ACKNOWLEDGMENTS

It is a pleasure to acknowledge the able technical assistance of R. Fergeau and J. F. Kepinski for setting up the mass spectrometer, M. Jacotin for the electronics and hardware, G. Le Scornet for the software, B. Rosenbaum for the data acquisition system, C. Vialle for setting up the laser, J. Biderman for the special devices for neutralization and ionization, and R. Baronnet for building the reference atomic beam apparatus. We are indebted to the members of the ISOLDE group at CERN for providing high Rb yields and for their support and hospitality. One of us (S.B.) wishes to thank the Deutsche Forschungsgemeinschaft for a fellowship.

*Permanent address: University of Bonn, D-5300 Bonn, Germany.

†Permanent address: Service de Physique Atomique, Centre d'Etudes Nucléaires, Saclay, France.

[1] G. Huber, C. Thibault, R. Klapisch, H. T. Duong, J. L. Vialle, J. Pinard, P. Juncar, and P. Jacquinot, Phys. Rev. Lett. 34, 1209 (1975).

[2] G. Huber, F. Touchard, S. Büttgenbach, C. Thibault, R. Klapisch, H. T. Duong, S. Liberman, J. Pinard, J. L. Vialle, P. Juncar, and P. Jacquinot, Phys. Rev. C 18, 2342 (1978).

[3] G. Huber, F. Touchard, S. Büttgenbach, C. Thibault,

R. Klapisch, S. Liberman, J. Pinard, H. T. Duong, P. Juncar, J. L. Vialle, P. Jacquinot, and A. Pesnelle, Phys. Rev. Lett. 41, 459 (1978).
[4]S. Liberman, J. Pinard, H. T. Duong, P. Juncar, J. L. Vialle, P. Jacquinot, G. Huber, F. Touchard, S. Büttgenbach, A. Pesnelle, C. Thibault, R. Klapisch, and Collaboration ISOLDE, C. R. Acad. Sci. Ser. B286, 253 (1978).
[5]S. Liberman, J. Pinard, H. T. Duong, P. Juncar, P. Pillet, J. L. Vialle, P. Jacquinot, F. Touchard, S. Büttgenbach, C. Thibault, M. de Saint Simon, R. Klapisch, A. Pesnelle, and G. Huber, Phys. Rev. A 22, 2732 (1980).
[6]M. Epherre, G. Audi, C. Thibault, R. Klapisch, G. Huber, F. Touchard, and H. Wollnik, Phys. Rev. C 19, 1504 (1979).
[7]G. Huber, R. Klapisch, C. Thibault, H. T. Duong, P. Juncar, S. Liberman, J. Pinard, J. L. Vialle, and P. Jacquinot, C. R. Acad. Sci. Ser. B282, 119 (1976).
[8]H. T. Duong and J. L. Vialle, Opt. Commun. 12, 71 (1974).
[9]H. Kopfermann, *Nuclear Moments* (Academic, New York, 1958).
[10]P. Jacquinot and R. Klapisch, Rep. Prog. Phys. 42, 773 (1979).
[11]H. L. Ravn, S. Sundell, and L. Westgaard, Nucl. Instrum. Methods 123, 131 (1975).
[12]P. Juncar, and J. Pinard, Opt. Commun. 14, 438 (1975).
[13]G. H. Fuller, J. Phys. Chem. Ref. Data 5, 835 (1976).
[14]V. Shirley and C. M. Lederer in *Hyperfine Interactions Studied in Nuclear Reactions and Decay*, edited by E. Karlsson and R. Wäppling (Almquist and Wiksell, Stockholm, 1975), Vol. 2.
[15]A. Rosén and I. Lindgren, Phys. Scr. 6, 109 (1972).
[16]R. M. Sternheimer and R. F. Peierls, Phys. Rev. A 3, 837 (1971).
[17]K. Heilig and A. Steudel, At. Data Nucl. Data Tables 14, 613 (1974).
[18]J. Bauche, private communication.
[19]W. Fischer, private communication to Heilig and Steudel (Ref. 17).
[20]F. A. Babushkin, Zh. Eksp. Teor. Fiz. 44, 1661 (1963) [Sov. Phys.—JETP. 17, 1118 (1963)].
[21]C. Bréchignac, S. Gerstenkorn, and P. Luc, Physica (Utrecht) 82C, 409 (1976).
[22]G. Fricke, private communication.
[23]H. Gerhardt, E. Matthias, H. Rinneberg, F. Schweider, A. Timmermann, R. Wenz, and P. J. West, Z. Phys. A 292, 7 (1979).
[24]R. Neumann, F. Träger, F. Kowalski, and G. zu Putlitz, Z. Phys. A 279, 249 (1976).
[25]H. W. Brandt, K. Heilig, H. Knöckel, and A. Steudel, Z. Phys. A 288, 241 (1978).
[26]H. D. Wohlfahrt, E. B. Shera, M. V. Hoehn, Y. Yamazaki, G. Fricke, and R. M. Steffen, Phys. Lett. 73B, 131 (1978).
[27]See Ref. 10, p. 786.
[28]W. D. Myers, Phys. Lett. 30B, 451 (1969); *Droplet Model of Atomic Nuclei* (Plenum, New York, 1977).
[29]*Table of Isotopes*, edited by C. M. Lederer and V. Shirley, 7th ed. (Wiley, New York, 1978).
[30]P. H. Stelson and L. Grodzins, Nucl. Data Tables A1, 21 (1965).
[31]L. Grodzins, Phys. Lett. 2, 88 (1962); J. Meyer-Ter-Vehn, Nucl. Phys. A249, 111 (1975); A249, 141 (1975).
[32]I. Angeli, and M. Csatlos, Nucl. Phys. A288, 480 (1977).
[33]I. Angeli, M. Beiner, R. Lombard, and D. Mas, J. Phys. G 6, 303 (1980).
[34]X. Campi and M. Epherre, Phys. Rev. C 22, 2605 (1980).
[35]F. Ackermann, I. Platz, and G. zu Putlitz, Z. Phys. 260, 87 (1973).
[36]E. Nolte and P. Vogt, Z. Phys. A 275, 33 (1975).
[37]E. Nolte, Y. Shida, W. Kutschera, R. Prestele, and H. Morinaga, Z. Phys. 268, 267 (1974).
[38]H. Wollnik, F. K. Wohn, K. D. Wünsch, and G. Jung, Nucl. Phys. A291, 355 (1977).
[39]R. E. Azuma, G. L. Borchert, L. C. Carraz, P. G. Hansen, B. Jonson, S. Mattsson, O. B. Nielsen, G. Nyman, I. Ragnarsson, and H. L. Ravn, Phys. Lett. 86B, 5 (1979).
[40]I. Ragnarsson, Symposium on Future Directions in Studies of Nuclei far from Stability, Nashville, Tennessee (1979).
[41]C. Ekström, S. Ingelman, G. Wannberg, and M. Skarestad, Nucl. Phys. A311, 269 (1978).
[42]C. Ekström, L. Robertsson, G. Wannberg, and J. Heinemeier, Phys. Scr. 19, 516 (1979).